Composites Part B 160 (2019) 1–9

Contents lists available at ScienceDirect

Composites Part B

journal homepage: www.elsevier.com/locate/compositesb

Self-polarized electrospun polyvinylidene fluoride (PVDF) nanofiber for sensing applications

Ehsan Ghafari[a], Na Lu[a,b,c,*]

[a] Lyles School of Civil Engineering, Sustainable Materials and Renewable Technology (SMART) Lab, Purdue University, USA
[b] School of Materials Engineering, Purdue University, USA
[c] Birck Nanotechnology Center, Purdue University, USA

ARTICLE INFO

Keywords:
PVDF
Piezoelectric
Nanofiber
Acoustic sensor

ABSTRACT

This study aimed at synthesizing a self-polarized electrospun PVDF which eliminates a need for the post treatment process. In addition, the feasibility of using an electrospun PVDF sensor for both active and passive sensing applications has been studied. The pitch-catch approach was considered for an active sensing approach while an acoustic emission monitoring was used as a passive method. Moreover, the experimental program involved studying the several parameters such as the transmitted signal amplitude, frequency and the distance on the received signal by PVDF sensor. The PVDF sensor was found to be effective in detecting the pulsed and continuous generated Lamb wave. The results indicate that the PVDF device is efficient in detecting the transmitted signal from 1 to 100 kHz, but less efficient either at a low-frequency range (< 1 kHz) or the higher range of frequency (> 100 kHz). The results clearly indicate that the sensor can detect different magnitudes of surface acoustic waves propagating on the surface.

1. Introduction

The effective structural health monitoring methods have gained more attention due to its critical role in detecting the premature failure and reducing the cost and time of maintaining structures. The piezoelectric devices have proved the capability of sensing in a variety of structural health monitoring applications such as detecting cracks, corrosion, strain sensing, etc. [1–14]. The most common type of piezoelectric sensors is ceramics based materials such as lead zirconate titanate (PZT) [15–18], which has been widely used in structural health monitoring applications in civil engineering infrastructure [19]. The major drawback of PZT, however, is their inherent brittleness so that they can only accommodate a very small strain level. This is a major obstacle for the use of these materials either in into flexible electronic devices or in high strain level applications, such as civil infrastructure.

The polymer-based nanofibers on the other hands have shown good piezoelectric properties to harvest the mechanical force under high strain conditions, due to their high flexibility potential and process simplicity as compared to ceramic materials. Among the known piezoelectric polymer materials, polyvinylidene fluoride (PVDF) is the only commercial product used as a piezoelectric material, due to its high flexibility, high piezoelectric properties, and good mechanical properties [20,21]. The voltage coefficient of PVDF is 10 times higher than of ceramic materials which makes it an exceptional candidate for sensing applications [22,23]. Also, PVDF polymer shows much lower acoustic impedance than ceramic crystals, which make them suitable for acoustic sensing applications [22–24].

Recently, the researchers have studied the feasibility of using PVDF sensor for both active and passive sensing applications [25–27]. Meyers et al. [28] studied the feasibility of using a the PVDF-ZnO nanocomposite for active sensing and damage detection. A good correlation between the damage index and the level of the applied force was obtained which shows the efficiency of PVDF-ZnO nanocomposite to be used as transducers for structural health monitoring and damage detection. Dodds et al. [29] used a PVDF-ZnO nanocomposite to detect the impact surface wave. The PVDF-ZnO was found to be effective in detecting the surface waves generated due to the impact force. Rosa et al. [24] investigated using PVDF as an acoustic emission sensor to detect the in situ damage of glass/epoxy laminates. The results indicated that the PVDF sensor can be used as an acoustic sensor in real-time monitoring of composite laminates for detecting different levels of structural damages of composite materials. Wang et al. [30] reported the PVDF acoustic sensor has a similar sensitivity to PZT. Yu et al. [31] developed a transducer consists of a PVDF-carbon nanotube (CNT) nanocomposite. The results indicated that the acoustic PVDF-CNT transducers can work as both acoustic actuators and sensors. The previous study by authors

* Corresponding author. Lyles School of Civil Engineering, Sustainable Materials and Renewable Technology (SMART) Lab, Purdue University, USA.
E-mail address: luna@purdue.edu (N. Lu).

https://doi.org/10.1016/j.compositesb.2018.10.011
Received 16 September 2018; Received in revised form 2 October 2018; Accepted 2 October 2018
Available online 03 October 2018
1359-8368/

confirmed the piezoelectric properties of the electrospun PVDF for sensing applications [32]. However, most of the PVDF composites have undergone a post-treatment process to promote the electroactive β-phase. The β-phase of PVDF is responsible for its electroactive properties such as ferroelectric, piezoelectric and pyroelectric properties. It has been reported that the sensitivity of PVDF sensors is related to the content of β-phase so that the higher β-phase will result in a better sensitivity of the sensor [33–36]. Hence, the enhancement of β-phase of PVDF is a critical step for making an efficient PVDF piezoelectric sensor. Despite several efforts, it is still a challenge to fabricate a PVDF sensor with high β-phase content due to the complication of the required post-treatment process.

To this end, the objective of this paper is twofold. Firstly, to synthesis and characterize a self-polarized electrospun PVDF which eliminates a need for the post-treatment process. The electrospinning method was used in this study to synthesize the piezoelectric nanofiber composite, making it considerably more attractive for commercial industrial and civil engineering applications. A proposed optimization model by Ghafari et al. [32] was used to achieve a bead-less PVDF nanofiber with the maximum fraction of the β-phase.

Secondly, to investigate the feasibility of using a self-polarized electrospun PVDF sensor for both active and passive sensing application. The pitch-catch approach was considered for the active sensing approach. Acoustic emission monitoring was also considered as a passive method which can detect the defects and cracks in structures by capturing the acoustic waves generated due to crack opening and propagation. Moreover, the experimental program involves studying the several parameters such as the transmitted signal amplitude, frequency and the distance on the received signal by PVDF device.

2. Experimental procedure

2.1. Materials characterization

PVDF pellet (Mw = 275,000), N,N-dimethylformamide (DMF, Sigma 99.5%), and acetone (Sigma, 99.7%) were purchased from Sigma-Aldrich. The multi objective optimization model was used to determine the PVDF concentration, DMF/acetone, voltage and flow rate [32]. PVDF solution was prepared by dissolving PVDF pellets at 27 (w/v %) concentration in solvent mixtures of DMF/acetone (1.5 v/v). The solution was heated at 70 °C for 1 h followed by 5 h stirring at room temperature. The homogenous PVDF solution was then added to the 10-ml plastic syringe which was placed in a syringe pump. The positive voltage of 12 kV was applied to the needle and the feeding rate of the solution was 0.2 mL/h. The nanofibers were spawned on a grounded rotating drum collector, which was placed at 10 cm from the tip of the needle. The electrospun PVDF nanofiber was compared to a spin coated sample to determine the fraction of beta phase of each electrospun PVDF sample using Fourier transform infrared spectroscopy (FTIR).

2.2. Sensor fabrication

The interdigitated electrode device (IDE) has been widely used for the fabrication of sensors and energy harvester [37]. The electrode pattern can be optimized in such a way to match the frequency of the mechanical vibration [38]. In this paper, an IDE-device is fabricated using an inkjet printing method. The inkjet printing has been used recently to print the flexible devices such as MEMS device [39,40], the light guide plate of a display [41] and flexible chemical sensor [42,43]. A piezoelectric-based Dimatix inkjet printer (DMP-2850) was used to deposit the silver electrode on the flexible substrate. In this study, a commercial silver ink (Centrix JS-B25HV) was used to deposit the conductive electrode on a PET substrate. The pattern was drawn and edited using the program of the printer. The experiments involved some trial deposition at the beginning in obtaining the appropriate resolution and thickness of the conductive layer. This process was controlled by using the waveform editor which alter the electrical pulse properties to optimize the ink droplets.

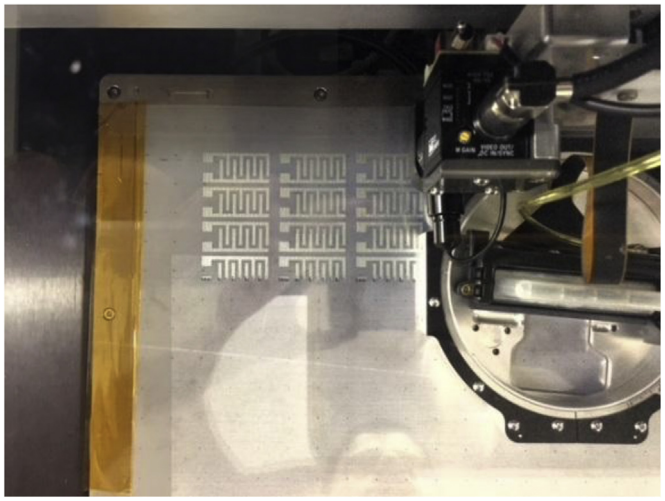

Fig. 1. The inkjet printer process from above.

The PET substrate was used in this study to fabricate the flexible PVDF device. The PET substrate was cleaned by soaking the substrate in toluene, acetone, isopropanol and for 5 min each and rinsed with DI water at the end. After optimizing the parameters of the waveform by executing the trial printing. The piezoelectric head was excited so that the deflection of the piezo head induces a pressure to expel the ink out of the nozzle. The multiple patterns were printed at the same time. The resolution of the printed pattern depends on several parameters such as ink properties, substrate, and the droplet size. The inkjet printing software allowed to deposit the multiple electrode patterns on the substrate. Fig. 1 shows the inkjet process from the top view and front view. This printer can create and define patterns over an area of about 200 × 300 mm and handle substrates up to 25 mm thick with an adjustable Z height. The IDE pattern then adhered on the drum collector during the electrospinning process. This allows the electrospun PVDF nanofiber to be deposited directly on the silver electrode. In order to enhance the durability of the PVDF device, the IDE along with the electrospun PVDF nanofiber was covered by a PDMS layer. The wires were then connected using the silver epoxy. The final piezoelectric device is shown in Fig. 2.

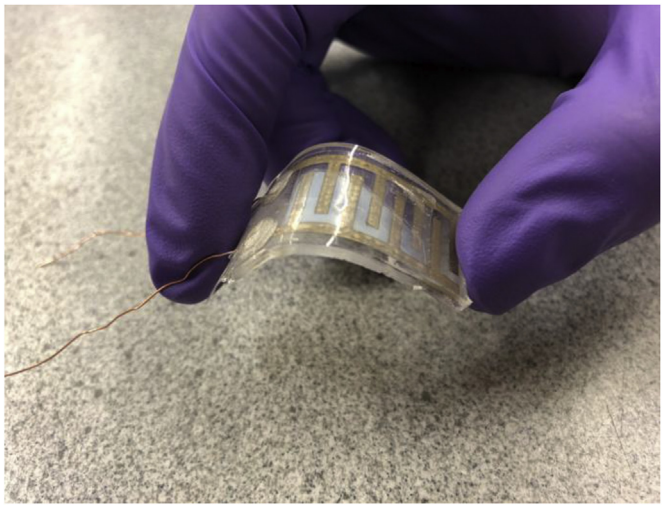

Fig. 2. The piezoelectric IDE device encapsulated in PDMS.

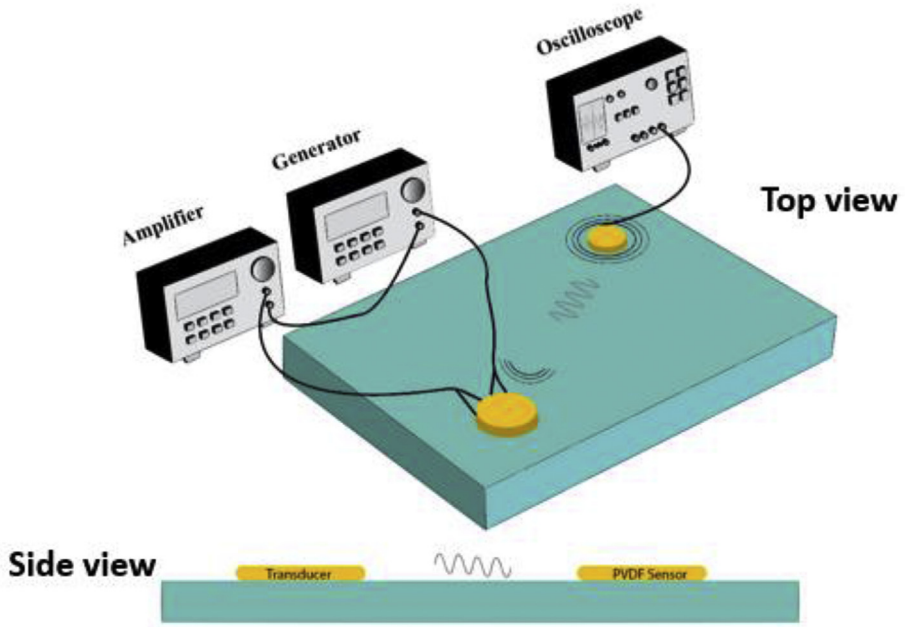

Fig. 3. The schematic of the pitch-catch system.

2.3. Experimental set-up

The pitch-catch set-up was used to study the potential of using the developed electrospun PVDF device as a receiver in a pitch-catch system to detect the Lamb wave. A pitch-catch system was set up in the lab to assess the efficiency of the flexible PVDF device for sensing application. In this approach, a PZT piezoelectric transducer acts as an actuator to propagates the Lamb waves while a PVDF piezoelectric device works as a sensor to detect the signal. The transducer is excited using a function generator to produce the Lamb wave. The transmitted signal is amplified using an AC signal amplifier. The received voltage by the piezoelectric sensor is also recorded by using an oscilloscope. The schematic of the pitch-catch system is shown in Fig. 3.

The initial received signal was recorded as the baseline which can be continuously compared with the later received signal from the sensor to assess the properties of the structures. In fact, the received signal will be changed due to any change in the host structures which can be related to the properties and physical change of the structures. Both the PZT transducer and PVDF piezoelectric sensor were attached to a wooden surface work table using a two-component adhesive, 3M's DP 460 Epoxy.

3. Results and discussion

3.1. Polarization characterization

The ferroelectric and piezoelectric properties of PVDF nanofiber are attributed to the fraction of the β phase. FTIR analysis is mostly used to quantify the electroactive phase content of PVDF. Assuming that FTIR absorption follows the Lambert-Beer law, the relative fraction of the β phase in a sample containing just α and β PVDF is (Eq. (1)) [44]:

$$F_\beta = \frac{A_\beta}{(K_\beta/K_\alpha)A_\alpha + A_\beta} \quad (1)$$

where F(β), represents the phase content; A_α and A_β are the absorbance at 766 and 840 cm^{-1}; K_α and K_β are the absorption coefficients at the respective wavenumber, which values are 6.1×104 and $7.7 \times 104\ cm^2\ mol^{-1}$, respectively.

Fig. 4 shows the FTIR spectra of electrospun PVDF and spin coating PVDF composite. As can be seen, electrospun PVDF sample exhibited a lower relative intensity of α peak, implying the transition from α phase to β phase in electrospun PVDF nanofiber composite. A clear shift in absorption band at 840 cm^{-1} for electrospun PVDF composites, indicate the presence of β phase. The FTIR data was also used to quantify the electroactive phase content of PVDF using Eq. (1). The fraction of β-phase in electrospun PVDF was found to be 75% which has increased up to 41% as compared to the one in the spin-coated sample. In fact, the PVDF nanofiber experiences an intense stretching force as collected on the drum which may lead to a similar effect to that of the mechanical stretching process. Also, applying high electrical field during the electrospinning processes helps to orient the polar dipoles in PVDF structure. This process can be analogs to the electrical poling process. Therefore, it can be concluded that the electrospinning process promotes the formation of β-phase without any need for post-treatment processes including electric poling and mechanical stretching.

3.2. Active and passive sensing

The structural health monitoring system includes active sensing and passive sensing methods. The passive sensing process does not depend on the external power source while the active sensing requires an external source of power to operate. The active sensing is the most common type of health monitoring systems to assess the condition of the structures by providing the real-time information about the structural performance, deterioration, strain, etc. Among them, the pitch-catch is one of the most efficient active sensing methods which has recently gained more attention in a variety of the engineering field [45–47]. The acoustic emission technique is a widely used passive technique in structural health monitoring.

To evaluate the feasibility of a PVDF sensor to receive the Lamb wave, a continuous 160 Vpp sinusoidal signal was generated by a function generator and amplified using an AC amplifier as described previously. The frequency of the transmitted signal was fixed at 2 kHz. Fig. 5 shows the transmitted signal along with the representative voltage-time plot as measured by electrospun PVDF device. It can be seen that the sensor successfully detected the propagated Lamb wave. The distance between the transducer and sensor was fixed at 15 cm. The maximum peak of 0.6 V has been detected by the PVDF sensor. The effect of the transducer-receiver distance was also considered to determine the degree of the transmitted signal's attenuation.

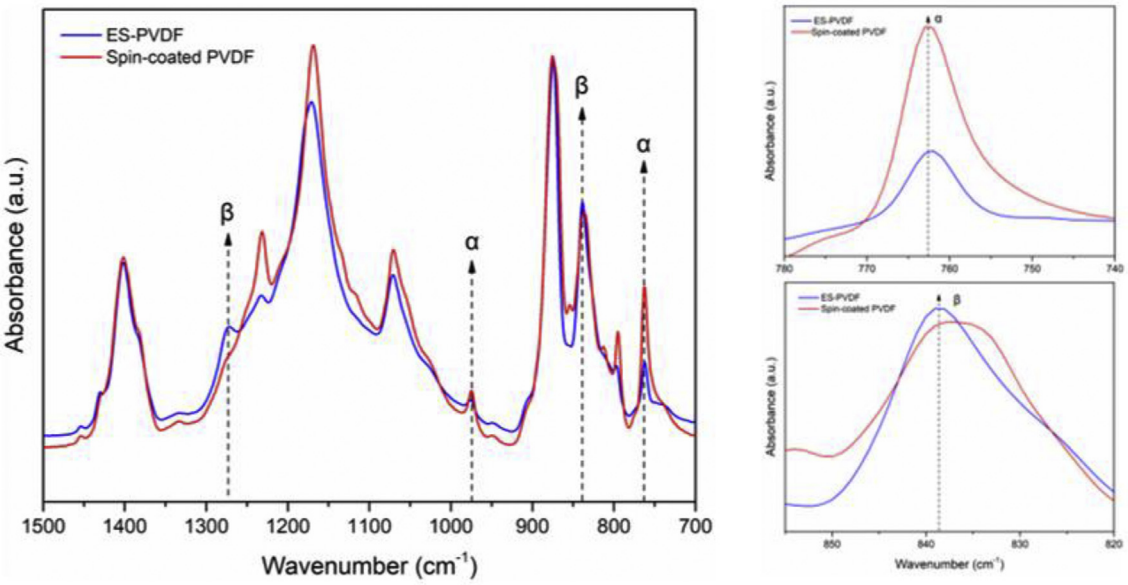

Fig. 4. FT-IR spectra of electrospun PVDF and spin coating PVDF composite. The absorbance peak at 766 and 840 cm^{-1} are the main peaks which represent the α and β phase of PVDF, respectively.

In order to compare the efficiency of the PVDF sensor at different active sensing situation, a relative parameter is defined as follow:

$$R/T(\%) = \frac{\text{The amplitude of the recieved signal}}{\text{The amplitude of the transmitted signal}} \quad (2)$$

In fact, the R/T can be an indication of the efficiency of the PVDF sensor in detecting the generated signal by the transducer.

The analysis of the parameters of the PVDF sensor efficiency was conducted in different steps. At the first step, the effect of the transmitted signal's amplitude on the received signal and R/T was assessed. In this experiment, the transducer was attached to the surface using the same procedure as previously explained in this section. The outcome of this experiments can assist in determining the most effective parameters for enhancing the efficiency of the PVDF sensor. The frequency of the transmitted signal varied from a very low frequency (< 100 Hz), to the high range frequency (> 100 kHz). Also, the amplitude of the transmitted signal varied from 40 Vpp to 200 Vpp. The effect of the amplitude and frequency of the transmitted signal was evaluated at three different distances of 15 cm, 50 cm, and 100 cm. Fig. 6 shows the variation of the R/T and the PVDF sensor voltage over the range of the amplitude of the transmitted signal. The amplitude of the transmitted signal varied from 40 Vpp to 200 Vpp, while the frequency of the transmitted signal was fixed at 2 kHz. The peak voltage of the PVDF sensor was recorded at 100 cm away from the transducer. As can be seen, the increase in the amplitude of the transmitted signal leads to an increase in the voltage of the PVDF sensor. Although the value of the received signal is influenced by the amplitude, no significant change can be observed in R/T value by changing the amplitude. The results indicated that the efficiency of the PVDF sensor in detecting the signal is not sensitive to the amplitude of the transmitted signal.

The efficiency of the PVDF sensor was also assessed to detect the Lamb wave at different distances. In this scope, the distance between

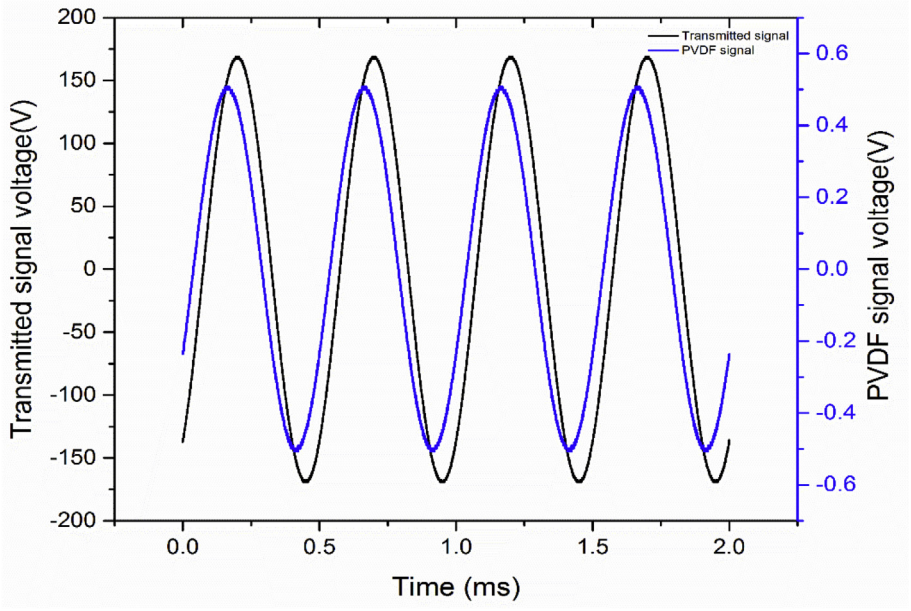

Fig. 5. The generated Lamb wave and the received signal by the PVDF sensor. The PVDF sensor successfully measured the propagated Lamb wave.

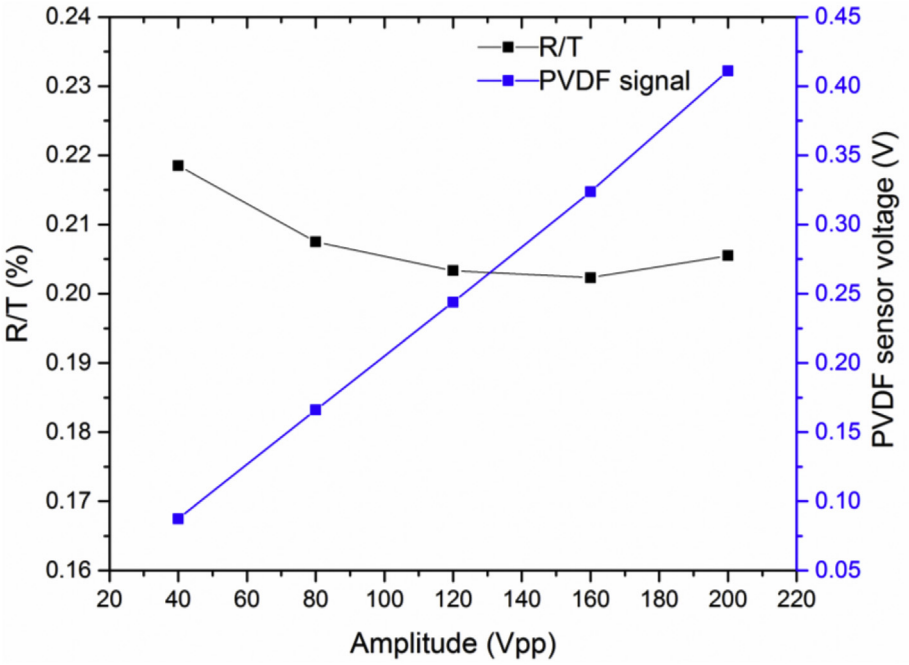

Fig. 6. The variation of the R/T and the PVDF sensor voltage over the range of the amplitude of the transmitted signal at 100 cm.

the sensor and transducer was varied by adjusting the position of the electrospun PVDF sensor from the transducer.

Fig. 7 summarizes the obtained R/T values over the three distances of 15 cm, 50 cm, and 100 cm as a function of the transmitted signal's amplitude. As shown, the R/T values drop as the distance increased. When the signal is transmitted at the lowest amplitude (40 Vpp), the highest R/T value at the distance of 100 cm was 0.21 which is 16% and 33% lower than the R/T ratio at the distance of 50 and 15 cm, respectively. In this case, the drop rate in R/T is 0.3% per cm. However, the signal is transmitted at the lowest amplitude (200 Vpp), the R/T value was dropped by 16% and 33% which gives almost the same value of drop rate (0.3% per cm). These results indicate that the amplitude of the transmitted signal does not affect the R/T value. It means that the efficiency of the PVDF sensor in detecting the Lamb wave signal is not affected by the amplitude of the transmitted signal. At a certain distance, the standard deviation of the R/T value for all the signal

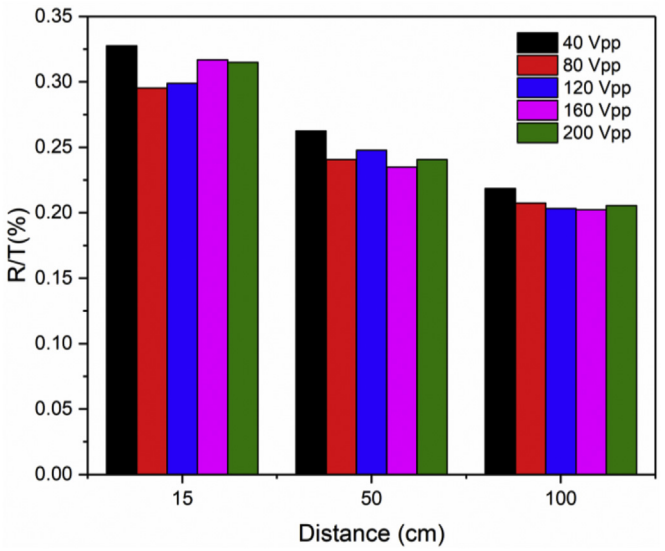

Fig. 7. A variation of R/T over the three distances of 15 cm, 50 cm, and 100 cm as a function of the transmitted signal's amplitude.

amplitude was calculated to assess the effect of the amplitude's signal on the efficiency of the PVDF sensor. The standard deviation of R/T value at 100 cm was found to be 0.0065 which is 38% and 52% lower than the standard deviation at the distance of 50 cm and 15 cm, respectively. The results clearly indicate that the effect of the transmitted signal's amplitude on the efficiency of the PVDF device is less pronounced at the higher distance away from the transducer. According to the obtained results, one can conclude that the amplitude of the transmitted signal doesn't affect the efficiency of the PVDF sensor in detecting the transmitted signal, while the efficiency of the PVDF sensor to detect the transmitted signal is highly affected by the distance between the transducer and receiver.

The second part of the experiment involves evaluating the efficiency of the PVDF sensor for detecting the signal for the wide range of frequency. In this scope, the amplitude of the transmitted signal was fixed at 160 Vpp, while the frequency varied from 5 Hz to 500 kHz. The received voltage by PVDF was recorded at three distances of 15 cm, 50 cm and 100 cm away from the transducer. Fig. 8 shows the PVDF signal voltage and the R/T value at 15 cm away from the transducer over a wide frequency range. As can be seen, both PVDF voltage signal and R/T curves follow almost the same trend. As the frequency is increased up to 1 kHz, R/T value is shown to increase sharply. The same level of R/T value was obtained in the frequency range of 1–100 kHz, while an abrupt decrease in R/T value can be observed for the frequency over 100 kHz. The effect can be better seen in the 3D curve of R/T as a function of the amplitude and frequency in Fig. 9. When the PVDF sensor was placed at 15 cm away from the transducer, the lowest R/T value was 0.022 for at the frequency of 50 Hz. This value was 93% lower than the maximum R/T value at the frequency of 100 kHz. The difference between the maximum and minimum of R/T was 93% and 95% for the distance of 50 and 100 cm, respectively. The results indicate almost the same rate as the increase in R/T value regardless of the distance between the transducer and the PVDF device. Fig. 10 shows the variation of R/T value over the frequency range as a function of the distance. As shown as the distance increases the R/T value drops, regardless of the frequency range.

At the frequency of 50 Hz, the R/T value for the sensor at 100 cm away from the transducer was 16% and 45% lower than the R/T ratio at the distance of 50 and 15 cm, respectively. However, the frequency of

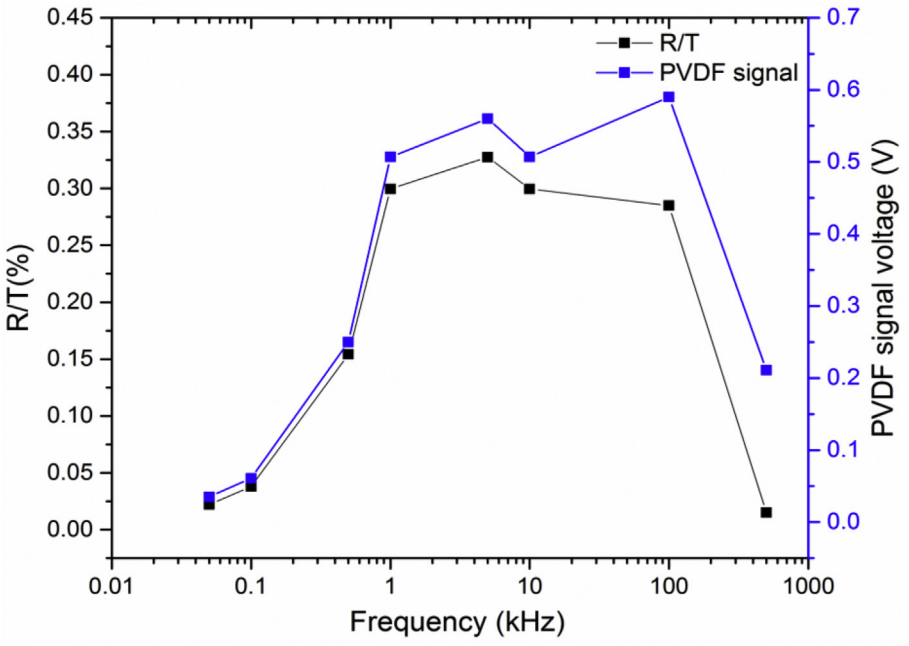

Fig. 8. The PVDF signal voltage and the R/T value over the frequency range.

100 kHz, the R/T value was 0.22 transducer which is 15% and 21% lower than the R/T ratio at the distance of 50 and 15 cm, respectively. Therefore, the effect of the distance on the efficiency of the sensor is more pronounced at the low-frequency range. It can be seen that the R/T ratio starts to decay at a higher frequency which can be due to the insufficient time for the PVDF nanofiber to be recovered from the induced strain.

The results indicate that the PVDF device is less efficient in detecting the transmitted signal either at a low-frequency range (< 1 kHz) or the higher range of frequency (> 100 kHz). One can note that an optimized range of the frequency needs to be determined to maximize the efficiency of the PVDF device in detecting the transmitted signal. As shown above, a range of 1 kHz–100 kHz can be considered as an optimized range to enhance the efficiency of the PVDF sensor. This range is considered as an acoustic range. Hence, a more experimental was planned to evaluate the feasibility of the PVDF sensor to be used as an acoustic sensor.

The previous results proved the efficiency of the PVDF device in detecting the transmitted signal for a wide frequency range of 1 kHz–100 kHz. The results suggest of using this sensor for acoustic emission as a passive system and in the echo-pulse system as active testing in health monitoring of the structures. In this scope, a series of the experiments were conducted aiming to evaluate the feasibility of the PVDF device to be used as an acoustic sensor.

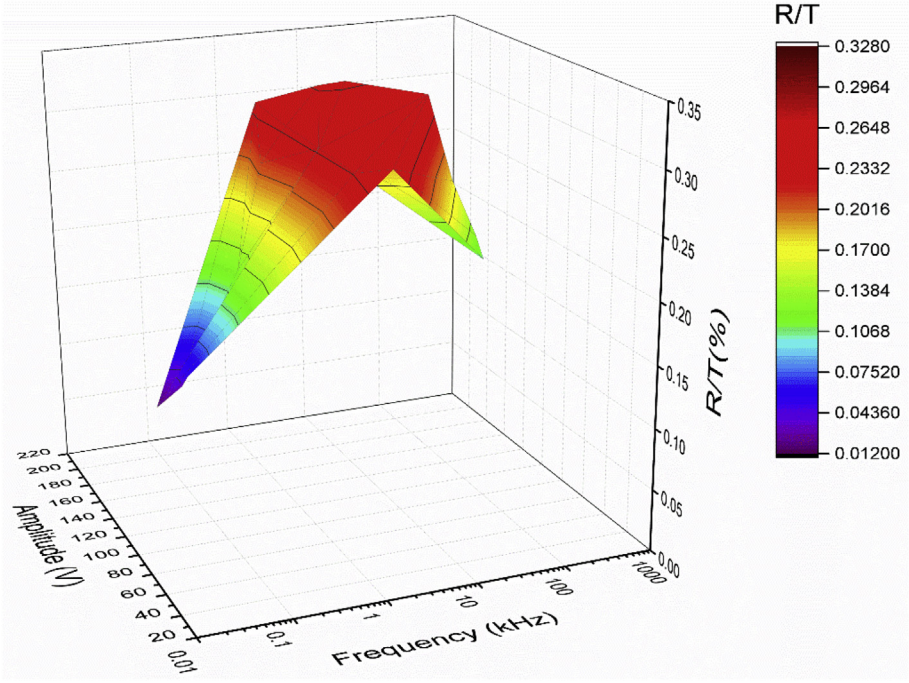

Fig. 9. The 3D curve of R/T as a function of the amplitude and frequency.

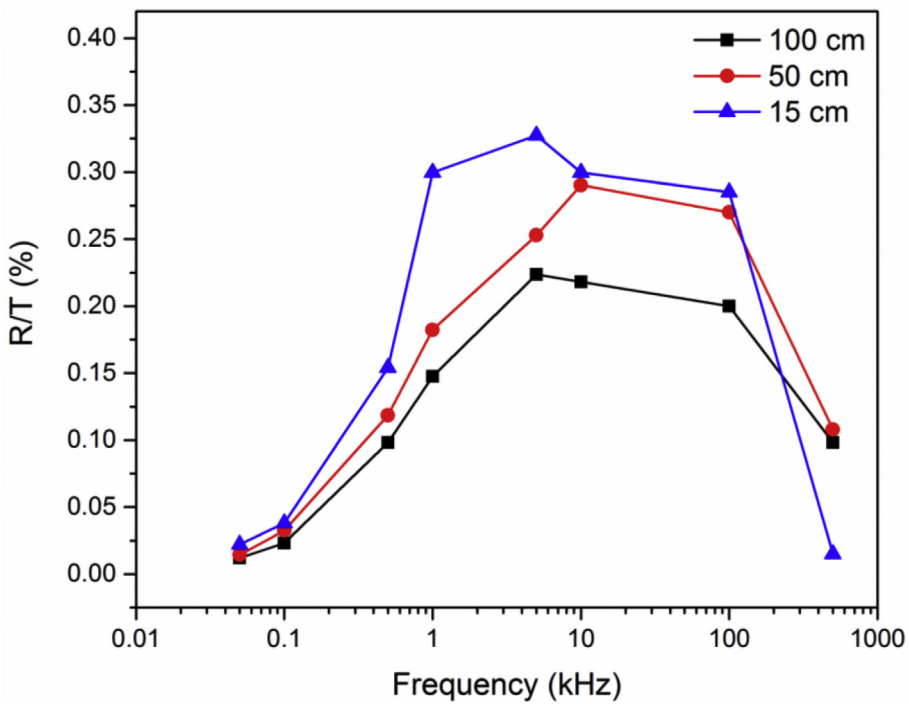

Fig. 10. The variation of R/T value over the frequency range as a function of the distance.

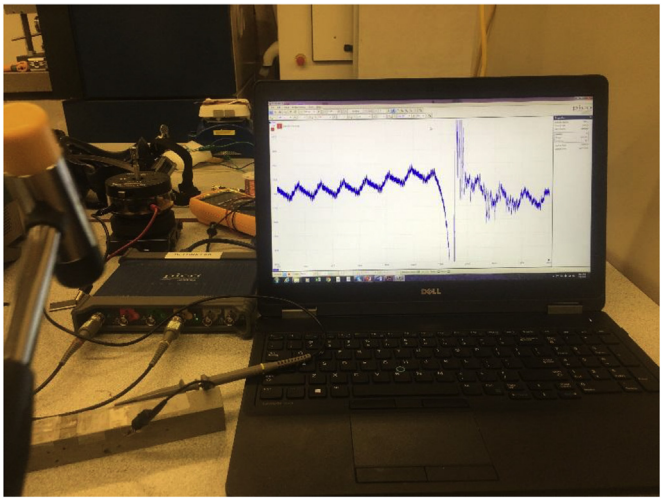

Fig. 11. The experimental setup for the acoustic emission test on cement paste beam.

The feasibility of the PVDF device in detecting the acoustic emission wave was evaluated on cement paste beam. In this scope, a hammer has been used to generate acoustic waves by periodic striking on the surface of a concrete beam. The viability of using PVDF sensor to detect the signal was evaluated by recording the voltage output using an oscilloscope. Fig. 11 shows the experimental setup for the acoustic emission test on cement paste beam. It should be noted that the higher impact energy increases the voltage response measured by the PVDF sensor. Therefore, a digital sound meter was used to record the generated sound by a hammer. Fig. 12 shows the voltage-time history responses of electrospun PVDF device mounted on the same substrate in which the peaks of positive and negative voltage outputs are recorded.

The sound level of 86–89 dB was generated by each impact force. The generated surface acoustic waves have been monitored and detected using the electrospun PVDF device. These results clearly indicate that the sensor can detect different magnitudes of acoustic waves propagating on the surface. The higher of the impact energy applied to the concrete, the higher the voltage generated by electrospun PVDF acoustic emission sensor. During the experiment, the voltage reached ~100 mV and disappeared quickly due to the low power generated by the electrospun PVDF sensor. The voltage output reached up to 100 mV which is incomparable to previous research results [48].

In summary, the PVDF sensor exhibits promising potential for both active and passive health monitoring system. The results indicate that the PVDF sensor can detect the generated Lamb wave which enables this device to be used to characterize the properties of the structural element. Also, the detection of the crack and structural defects can be determined using the pitch-catch method. The feasibility of using PVDF device as an acoustic sensor was also proved by conducting experiments on a cement paste beam. The results prove that the PVDF sensor can detect the acoustic emission wave.

4. Conclusion

A self-polarized electrospun PVDF with a considerable fraction of β phase was synthesized. The feasibility of using a self-polarized electrospun PVDF sensor for both active and passive sensing application was investigated. In summary, the PVDF sensor exhibits promising potential for both active and passive health monitoring system. The results indicate that the PVDF sensor can detect the generated Lamb wave which enables this device to be used to characterize the properties of the structural element. Also, the detection of the crack and structural defects can be determined using the pitch-catch method. The feasibility of using PVDF device as an acoustic sensor was also proved by conducting experiments on a cement paste beam. The results prove that the PVDF sensor can detect the acoustic emission wave. A series of experiments were conducted to evaluate the effect of several parameters of the transmitted signal such as amplitude and frequency on the received signal. The effect of transducer-sensor distance was also considered to evaluate the attenuation of the transmitted signal. The PVDF sensor was found to be effective in detecting the generated Lamb wave. It was found that the efficiency of the PVDF sensor in detecting the signal is not sensitive to the amplitude of the transmitted signal. Also,

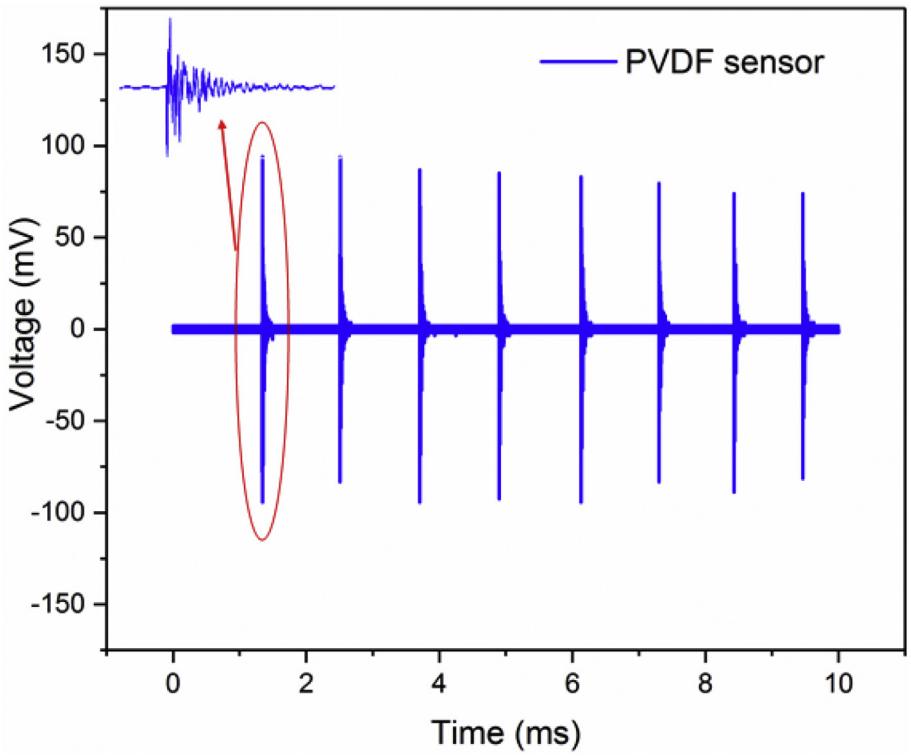

Fig. 12. The voltage generation as a result of the surface waves induced by the periodic striking of a grounded steel bar on the composite substrate.

the transmitted signal's amplitude has an insignificant effect on the attenuation rate of the transmitted signal over the distance. However, the efficiency of the PVDF sensor to detect the transmitted signal is highly affected by the distance between the transducer and the receiver. The results indicate that the PVDF device is less efficient in detecting the transmitted signal either at a low-frequency range (< 1 kHz) or the higher range of frequency (> 100 kHz). The optimized frequency was found to be in the range of 1 kHz–100 kHz to enhance the efficiency of the PVDF sensor. The efficiency of the PVDF sensor for detecting the acoustic wave was also studied by hammer impact testing. These results clearly indicate that the sensor is able to detect different magnitudes of surface acoustic waves propagating on the surface. The higher of the impact energy applied to the concrete, the higher the voltage generated by electrospun PVDF AE sensor. The results of this thesis can assist in adopting the electrospun PVDF piezoelectric sensor in a variety of sensing and energy harvesting applications in civil engineering infrastructure.

Acknowledgment

The authors at Purdue University are grateful to the funding supports from the National Science Foundation (NSF CMMI–1560834) and Indiana Department of Transportation (SPR-4210).

References

[1] Kon S, Oldham K, Horowitz R. Piezoresistive and piezoelectric MEMS strain sensors for vibration detection. Proc SPIE 2007;6529. 65292V-1.
[2] Zhao X, et al. Active health monitoring of an aircraft wing with embedded piezoelectric sensor/actuator network: I. Defect detection, localization and growth monitoring. Smart Mater Struct 2007;16(4):1208.
[3] Rathod V, Mahapatra DR. Ultrasonic Lamb wave based monitoring of corrosion type of damage in plate using a circular array of piezoelectric transducers. NDT E Int 2011;44(7):628–36.
[4] Feucht G, Schleicher A, Frank G. Piezoelectric gas sensor. Google Patents; 2001.
[5] Lu N, Ferguson I. III-nitrides for energy production: photovoltaic and thermoelectric applications. Semicond Sci Technol 2013;28(7):074023.
[6] Oza S, et al. Effect of surface treatment on thermal stability of the hemp-PLA composites: correlation of activation energy with thermal degradation. Compos B Eng 2014;67:227–32.
[7] Lu N, Oza S. Thermal stability and thermo-mechanical properties of hemp-high density polyethylene composites: effect of two different chemical modifications. Compos B Eng 2013;44(1):484–90.
[8] Lu N, Oza S. A comparative study of the mechanical properties of hemp fiber with virgin and recycled high density polyethylene matrix. Compos B Eng 2013;45(1):1651–6.
[9] Lu Y, et al. Recent developments in bio-monitoring via advanced polymer nanocomposite-based wearable strain sensors. Biosens Bioelectron 2018. https://doi.org/10.1016/j.bios/2018.08.037.
[10] Zhou B, et al. Continuously fabricated transparent conductive polycarbonate/carbon nanotube nanocomposite film for switchable thermochromic applications. J Mater Chem C 2018;6:8360–71.
[11] Guan X, et al. Carbon nanotubes-adsorbed electrospun PA66 nanofiber bundles with improved conductivity and robust flexibility. ACS Appl Mater Interfaces 2016;8(22):14150–9.
[12] Liu H, et al. Organic vapor sensing behaviors of conductive thermoplastic polyurethane–graphene nanocomposites. J Mater Chem C 2016;4(20):4459–69.
[13] Liu H, et al. Lightweight conductive graphene/thermoplastic polyurethane foams with ultrahigh compressibility for piezoresistive sensing. J Mater Chem C 2017;5(1):73–83.
[14] Song B, et al. Interfacially reinforced carbon fiber/epoxy composite laminates via in-situ synthesized graphitic carbon nitride (g-C3N4). Compos B Eng Feb 2019;158(1):259–68.
[15] Gu L, Cui Nuanyang, Cheng Li, Xu Qi, Bai Suo, Yuan Miaomiao, Wu Weiwei, Liu Jinmei, Zhao Yong, Ma Fei. Flexible fiber nanogenerator with 209 V output voltage directly powers a light-emitting diode. Nano Lett 2012;13(1):91–4.
[16] Zhang G, Xu Shiyou, Shi Yong. Electromechanical coupling of lead zirconate titanate nanofibres. IET Micro & Nano Letters 2011;6(1):59–61.
[17] Ghafari E, et al. Evaluation the compressive strength of the cement paste blended with supplementary cementitious materials using a piezoelectric-based sensor. Construct Build Mater 2018;171:504–10.
[18] Liu H, et al. Electrically conductive thermoplastic elastomer nanocomposites at ultralow graphene loading levels for strain sensor applications. J Mater Chem C 2016;4(1):157–66.
[19] Song G, Gu H, Li H. Application of the piezoelectric materials for health monitoring in civil engineering: an overview, in Engineering, Construction, and Operations in Challenging Environments. Earth Space 2004;2004:680–7.
[20] Harrison J, Ounaies Z. Piezoelectric polymers. Encyclopedia of Polymer Science and Technology 2002;3.
[21] Li Y, et al. 3-D magnetic graphene oxide-magnetite poly (vinyl alcohol) nanocomposite substrates for immobilizing enzyme. Polymer 2018;149(2018):13–22.
[22] Bauer S, Bauer F. Piezoelectric polymers and their applications. Piezoelectricity: evolution and future of a technology 2008;114:157–80.
[23] Xu J, et al. Microphone based on polyvinylidene fluoride (PVDF) micro-pillars and patterned electrodes. Sensor Actuator Phys 2009;153(1):24–32.
[24] De Rosa IM, Sarasini F. Use of PVDF as acoustic emission sensor for in situ

monitoring of mechanical behaviour of glass/epoxy laminates. Polym Test 2010;29(6):749–58.
[25] Ponnamma D, et al. Controlling the sensing performance of rGO filled PVDF nanocomposite with the addition of secondary nanofillers. Synth Met 2018;243:34–43.
[26] Sengupta D, et al. Characterization of single polyvinylidene fluoride (PVDF) nanofiber for flow sensing applications. AIP Adv 2017;7(10):105205.
[27] Lei K-F, et al. The structure design of piezoelectric poly (vinylidene fluoride)(PVDF) polymer-based sensor patch for the respiration monitoring under dynamic walking conditions. Sensors 2015;15(8):18801–12.
[28] Meyers FN, et al. Active sensing and damage detection using piezoelectric zinc oxide-based nanocomposites. Nanotechnology 2013;24(18):185501.
[29] Dodds JS, Meyers FN, Loh KJ. Enhancing the piezoelectric performance of PVDF-TrFE thin films using zinc oxide nanoparticles. Sensors and smart structures technologies for civil, mechanical, and aerospace systems, vol. 2012. International Society for Optics and Photonics; 2012.
[30] Wang Z, et al. The study of PVDF acoustic emission sensor. Nondestructive characterization of materials VIII. Springer; 1998. p. 647–52.
[31] Yu X, et al. Carbon nanotube-based transparent thin film acoustic actuators and sensors. Sensor Actuator Phys 2006;132(2):626–31.
[32] Ghafari E, Jiang X, Lu N. Surface morphology and beta-phase formation of single polyvinylidene fluoride (PVDF) composite nanofibers. Adv Comp Hybrid Mat 2018;1(2):332–40.
[33] Li B, et al. Sensitivity of pressure sensors enhanced by doping silver nanowires. Sensors 2014;14(6):9889–99.
[34] Hosseini M, Makhlouf ASH. Industrial applications for intelligent polymers and coatings. Springer; 2016.
[35] Kumar A, Periman M. Simultaneous stretching and corona poling of PVDF and P (VDF-TriFE) films. II. J Phys Appl Phys 1993;26(3):469.
[36] Kaura T, Nath R, Perlman M. Simultaneous stretching and corona poling of PVDF films. J Phys Appl Phys 1991;24(10):1848.
[37] Duan WH, Wang Q, Quek ST. Applications of piezoelectric materials in structural health monitoring and repair: selected research examples. Materials 2010;3(12):5169–94.
[38] Gu H, Lloyd GM, Wang ML. Interdigitated PVDF transducer for Lamb wave generation and reception. Smart structures and materials. International Society for Optics and Photonics; 2005.
[39] Lessing J, et al. Inkjet printing of conductive inks with high lateral resolution on omniphobic “RF paper” for paper-based electronics and MEMS. Adv Mater 2014;26(27):4677–82.
[40] Silverbrook K. Inkjet printer comprising MEMS temperature sensors. Google Patents; 2006.
[41] Feng D, et al. Novel integrated light-guide plates for liquid crystal display backlight. J Optic Pure Appl Optic 2005;7(3):111.
[42] Huang L, et al. Graphene-based conducting inks for direct inkjet printing of flexible conductive patterns and their applications in electric circuits and chemical sensors. Nano Res 2011;4(7):675–84.
[43] Abe K, Suzuki K, Citterio D. Inkjet-printed microfluidic multianalyte chemical sensing paper. Anal Chem 2008;80(18):6928–34.
[44] Martins P, Lopes AC, Lanceros-Mendez S. Electroactive phases of poly (vinylidene fluoride): determination, processing and applications. Prog Polym Sci 2014;39(4):683–706.
[45] Giurgiutiu V. Tuned Lamb wave excitation and detection with piezoelectric wafer active sensors for structural health monitoring. J Intell Mater Syst Struct 2005;16(4):291–305.
[46] Diamanti K, Soutis C. Structural health monitoring techniques for aircraft composite structures. Prog Aero Sci 2010;46(8):342–52.
[47] Raghavan A, Cesnik CE. Review of guided-wave structural health monitoring. Shock Vib Digest 2007;39(2):91–116.
[48] Chen X, et al. Flexible piezoelectric nanofiber composite membranes as high performance acoustic emission sensors. Sensor Actuator Phys 2013;199:372–8.